Effects of 1,25-dihydroxyvitamin D_3 on the local bone renin-angiotensin system in a murine model of glucocorticoid-induced osteoporosis

LIN SHEN, CHEN MA, BO SHUAI and YANPING YANG

Department of Integrated Traditional Chinese and Western Medicine, Union Hospital, Tongji Medical College, Huazhong University of Science and Technology, Wuhan, Hubei 430022, P.R. China

Received January 23, 2016; Accepted February 10, 2017

DOI: 10.3892/etm.2017.4404

Abstract. Active vitamin D is closely related to the circulating renin-angiotensin system (RAS) in experimental animal models and humans; however, corresponding local bone data remain limited. The present study examined whether 1,25-dihydroxyvitamin D_3 supplementation altered local bone RAS elements in a murine model of glucocorticoid-induced osteoporosis (GIOP). A total of 36 8-week-old mice were randomized into three equal-sized groups: The sham, GIOP and 1,25-dihydroxyvitamin D_3 treatment groups. After 12 weeks, the cancellous bone microstructure of the third lumbar vertebra and left femur from the mice from each group were examined using micro-computed tomography. To access the impact of glucocorticoid use, the effect of 1,25-dihydroxyvitamin D_3 on cancellous bone microstructure, the expression of bone turnover markers, circulation and expression of the main RAS components was assessed. Results demonstrated that bone volume fraction, trabecular number and trabecular thickness of the treatment and sham groups were significantly higher than the GIOP group ($P<0.05$). Furthermore, the structure model index, trabecular separation and bone surface to bone volume ratio of the sham and treatment groups were significantly reduced compared with the GIOP group ($P<0.05$). All assessed parameters exhibited no significant differences between the treatment and sham groups. mRNA expression levels of local bone angiotensin type 1 and 2 receptors and receptor activator of nuclear factor-κB ligand were significantly lower in the treatment group than in the GIOP group ($P<0.05$); however, there were no significant differences in circulating protein levels between the groups ($P>0.05$). In conclusion, 1,25-dihydroxyvitamin D_3 may modulate bone metabolism by downregulating the local bone RAS in mice with GIOP.

Correspondence to: Dr Bo Shuai, Department of Integrated Traditional Chinese and Western Medicine, Union Hospital, Tongji Medical College, Huazhong University of Science and Technology, 1277 Jie Fang Avenue, Wuhan, Hubei 430022, P.R. China
E-mail: bobo3137@126.com

Key words: renin-angiotensin system, 1,25-dihydroxyvitamin D_3, osteoporosis, glucocorticoid, micro-computed tomography

Introduction

Glucocorticoid-induced osteoporosis (GIOP) is a common syndrome that may be a complication of immunosuppressive glucocorticoid (GC) therapy following organ transplantation or inflammatory disease (1,2). Dysfunctional bone metabolism is key in the pathogenesis of GIOP (3,4). It has been suggested that the renin-angiotensin system (RAS) regulates blood pressure and electrolyte homeostasis systemically (5). Local tissue-specific RASs have also been identified in various organs (6). A local RAS in bone, closely related to bone metabolism, has been defined previously (6). Research has demonstrated that angiotensin (Ang) II suppressed osteoblastic cell differentiation and bone formation by binding specifically to the Ang type 1 receptor (AT1R) *in vitro* (7). Both Ang I and II have been identified to stimulate osteoclastogenesis in osteoblast and osteoclast co-cultures, which was inhibited by treatment with an Ang-converting enzyme (ACE) inhibitor (8). This finding suggests that ACE converts Ang I to Ang II within osteoblasts or osteoclasts. A study by Liu *et al* (9) demonstrated that captopril dose-dependently inhibited ACE and subsequently increased the secretion of alkaline phosphatase and the mRNA expression level of collagen I in rat osteoblasts. Further research has indicated that Ang II promotes the differentiation and activation of osteoclasts indirectly by upregulating the receptor activator of nuclear factor-κB ligand (RANKL) in osteoblasts (10,11). In conclusion, these results indicate that a local RAS exists in bone that is associated with bone metabolism disorders characterized by reduced osteoblastic and enhanced osteoclastic activity.

The active metabolite of vitamin D, 1,25-dihydroxyvitamin D_3 [$1,25(OH)_2D_3$], and the vitamin D receptor (VDR) are important for normal biological activity in the body. Increased levels of RAS components are observed in the blood, heart, kidney and bone tissue in VDR or CYP2781 knockout mice (12). This is predominantly due to inhibition of the formation of $1,25(OH)_2D_3$ or inhibition of its biological

effects (12-14). Therefore, $1,25(OH)_2D_3$ is considered to be an important negative regulator of RAS, most likely via the inhibition of renin gene transcription (15,16). Furthermore, research involving VDR knockout mice and *in vitro* models has indicated that RAS activity may be directly inhibited through the vitamin D signaling pathway (17).

The present study investigated the effects of $1,25(OH)_2D_3$ on the systemic and local bone RAS using a murine model of GIOP. Specifically, the ability of $1,25(OH)_2D_3$ to improve the abnormalities in bone metabolism, associated with GIOP, by inhibiting RAS activity was examined.

Materials and methods

Ethics statement. All animal experiments were conducted in accordance with the recommendations of the Huazhong University of Science and Technology (Wuhan, China). The research protocol was approved by the Committee on the Ethics of Animal Experiments of the Huazhong University of Science and Technology.

Animal treatment and grouping. A total of 36 8-week-old specific pathogen-free C57BL/6 male mice (22-26 g in weight) were purchased from and maintained at the Experimental Animal Center of Huazhong University of Science and Technology (certificate no. 0237269; Hubei provincial experimental animal facility permit, SYXK 2010-0057). During the experiment, mice were housed in cages (temperature, 23±1˚C; relative humidity, 50-60%), had free access to food and water and were exposed to a 12-h light/dark cycle (6 a.m. to 6 p.m. darkness). All mice were kept under sterile conditions and provided with disinfected food and water for 1 month. Following this, the mice were randomized into three groups, with 12 mice per group. The groups were as follows: The GIOP; the sham; and the $1,25(OH)_2D_3$ treatment group. Mice in the GIOP and treatment groups received intramuscular injections of dexamethasone (DXM; 3 mg/kg body weight; Chengdu Tiantaishan Pharmaceutical Co., Ltd., Chengdu, China) twice weekly for 12 weeks. The sham group received intramuscular saline injections in the same way as the DXM injections. The treatment group also received $1,25(OH)_2D_3$, which was produced by R. P. Scherer GmbH & Co. KG (Eberbach, Germany); affiliated to Roche Pharma (Schweiz) Ltd. (Reinach, Switzerland); 0.7 μg/kg body weight) by intragastric gavage (18). The doses of DXM and $1,25(OH)_2D_3$ were selected based on a dose-response study carried out in a rat model of osteoporosis (18).

Mice were raised under consistent conditions with free movement. After 12 weeks, blood samples were taken and the animals were sacrificed. The third lumbar vertebra and left femur were immediately removed from each of the animals. Subsequently, muscle and soft tissue were detached from the bone and the bone samples were wrapped in saline-soaked gauze for further analysis.

Micro-computed tomography (CT) imaging. Imaging of the trabecular microstructure and three-dimensional (3D) imaging of the third lumbar vertebra and left femur were analyzed using micro-CT (μCT20; Scanco Medical, Bassersdorf, Switzerland), as previously described (19,20). Scans of bone samples were made along the longitudinal axis of the specimen. Scan parameters were as follows: 90 kV, 88 μA, 2˚ rotation step and a 360˚ rotation angle. Consecutive micro-CT scans were captured, including 100 lumbar vertebral slices and 250 left femur slices, at 14-μm thickness. The image size was 1,024x1,024 pixels. Image reconstruction was performed using a virtual machine system (Image Processing Language v. 5.0A; Scanco Medical) in cluster configuration with a voxel size of 14x14x14 μm (18). In order to obtain the original 3D images of the samples, a threshold value of 180 was used to binarize the spongiosa and bone marrow (20). A fixed threshold was used to determine the trabecular bone. Based on the consecutive slices, hand-drawn contours were used to isolate the metaphyseal region of interest and trabecular compartments. Bone micro-architecture was assessed with direct 3D methods as described previously (20). Morphometric parameters of the original 3D images were directly determined from the binarized volume of interest (21). The same explication of other related parameters was followed according to a previous study (20). The measurement precision was assessed using the coefficient of variation (CV), which was <4%.

Measurement of bone turnover markers and main RAS components. Blood samples were harvested at the end of the 12-week study period, centrifuged for 15 min at 1,000 x g at 2-8˚C and stored at -70˚C. Parameters for the test included serum calcium, inorganic phosphorous, and alkaline phosphatase, which were assessed by standard laboratory techniques (Roche Diagnostics GmbH, Germany). Bone turnover markers $1,25(OH)_2D_3$, β-Crosslaps (β-CTX) and total N-terminal propeptide of type I procollagen (T-PINP) were measured using Cobas E411C kits (Roche Diagnostics GmbH) at the same central biochemical laboratory using an automated Roche electrochemiluminescence system (Roche Diagnostics GmbH). The main RAS components (ACE and Ang II) were measured using kits (Abcam, Cambridge, UK; catalog nos. ab155452 and ab47831). Intra-assay and inter-assay CVs of the biochemical parameters, bone turnover markers and main RAS components were <3%.

Reverse transcription-quantitative polymerase chain reaction (RT-qPCR). Total RNA was extracted from lumbar vertebrae using TRIzol reagent (Invitrogen; Thermo Fisher Scientific, Inc., Waltham, MA, USA). After treatment with DNase I (Sigma-Aldrich; Merck KGaA, Darmstadt, Germany) to remove genomic DNA, cDNA was generated using a RevertAid First Strand cDNA synthesis kit (Thermo Fisher Scientific, Inc.). The following mixture was prepared for the RT step: 9.0 μl H_2O, 4.0 μl buffer (5X), 1.0 μl oligo (dT15), 2.0 μl target RNA solution, 2.0 μl dNTPs (10 mM), 1.0 μl RNase inhibitor and 1.0 μl reverse transcriptase, giving a total reaction volume of 20 μl. The reaction conditions for cDNA synthesis included incubation of tubes at 42˚C for 30 min followed by heat inactivation at 70˚C for 15 min. mRNA expression levels of ACE, Ang II, AT1R, Ang type 2 receptor (AT2R), osteoprotegerin (OPG) and RANKL were measured using a qPCR kit [FastStart Universal SYBR-Green 1 PCR master mix (Rox); Roche Diagnostics, Indianapolis, IN, USA] and the gene-specific primers demonstrated in Table I. The qPCR reaction mixture consisted of a total reaction volume

Table I. Primer sequences used for reverse transcription-quantitative polymerase chain reaction.

Target	Primer sequences (5'-3')
β-actin	F:CACCCAGCACAATGAAGATCAAGAT
	R: CCAGTTTTTAAATCCTGAGTCAAGC
OPG	F: CTTGCCCTGACCACTACTACAC
	R: CTCATTTGAGAAGAACCCATCTG
RANKL	F: AACATATCGTTGGATCACAGCAC
	R: GGACAGACTCACTTTATGGGAAC
AT1R	F: CCTAACTGGATGATTGGTGGAC
	R: GGTGACTTTGAGCGAAGGGTAT
AT2R	F: CACCCACCAAGTGTCCAATAA
	R: CAGCAGCAATCCCACATAAAC
Ang II	F: GCTAAGGACCCCACTGTTGCTA
	R:TGTAGATGCCATTCGTGGTGTG
ACE	F: TCTCGGTCTCCACTCCTGAACA
	R: AAGTGGGTTTCGTTTCGGGTA

F, forward primer; R, reverse primer; ACE, angiotensin-converting enzyme; Ang II, angiotensin II; AT1R, angiotensin II receptor type 1; AT2R, angiotensin II receptor type 2; RANKL, receptor activator of NF-kB ligand; OPG, osteoprotegerin.

of 20 μl that contained 2.9 μl H_2O, 1.0 μl cDNA sample, 5.0 μl 10X buffer, 7.0 μl 25 mM $MgCl_2$, 1.0 μl 10 mM dNTPs, 0.8 μl forward primer (20 pmol/ml), 0.8 ml reverse primer (20 pmol/ml), 1.0 μl SYBR-Green and 0.5 μl Taq (5 U/ml) (22). A real-time PCR system (ABI7300; Applied Biosystems; Thermo Fisher Scientific, Inc.) was used to run the following cycling conditions: 95˚C for 10 min; followed by 40 cycles at 95-60˚C for 15 sec, and the final extension at 60˚C for 5 min. Relative expression levels were normalized to the internal control β-actin according to the $2^{-\Delta\Delta Cq}$ method and three repeats were performed (22-25).

Immunohistochemistry. Immunohistochemical staining was performed using DAB kits (Beijing Zhongshan Golden Bridge Biotechnology Co., Ltd., Beijing, China). Briefly, tissue sections were immersed in xylene and rehydrated in a graded alcohol series and water for deparaffinization. The staining was blocked in 3% H_2O_2 in methanol for 5 min to quench endogenous peroxidase activity. Subsequently, slides were incubated with primary anti-Ang II (1:50; sc-20718; Santa Cruz Biotechnology, Inc., Dallas, TX, USA), and anti-ACE (ab11734; 1:100), anti-AT1R (ab92486; 1:1,000) and anti-AT2R antibodies (ab108252; 1:1,000) (all from Abcam, Cambridge, UK) overnight at 4˚C. Following this, slides were incubated with secondary goat antibody (ab191866; 1:1,000; Abcam) and horseradish peroxidase-labeled streptavidin (Wuhan Boster Biological Technology, Ltd., Wuhan, China; catalog no., BA1088) for 1 h at 4˚C (22). Subsequently, antibody binding was visualized using DAB-H_2O_2 solution. Stained tissues were mounted, following hematoxylin staining, and viewed under a light microscope (magnification, x400; Olympus Corp., Tokyo, Japan). Cells were counted as previously described (22). The anti-ACE, -Ang II, -AT1R and -AT2R labeling indices were calculated using the following formula: ACE labeling index = number of ACE-positive cells/total number of cells per high power field x 100 (22).

Cells were differentiated according to their morphological characteristics and one pathologist analyzed all samples. Osteoblasts were cuboidal mononuclear cells, attached to the bone matrix surface and lined the surface of trabecular bone. Osteoclasts were multinucleated cells. Osteocytes were mononuclear cells filling the bone lacunae of the trabecular. All cells in the bone marrow were defined as bone marrow cells, regardless of cell type (22).

Statistical analysis. Statistical analysis was performed using SPSS v.13.0 software (SPSS, Inc., Chicago, IL, USA). Kruskal-Wallis tests, analysis of variance and Tukey's multiple comparison tests were used to determine whether significant differences existed between the groups. Data were presented as the mean ± standard deviation, unless otherwise stated. $P<0.05$ was considered to indicate a statistically significant difference.

Results

Survival outcomes, effects on body weight and serum biochemical parameters. One mouse in the GIOP group died due to a bite from another mouse. All other mice survived until they were sacrificed. The final body weight of mice was significantly lower in the sham and treatment groups than those in the GIOP group (both $P<0.05$; Table II). Serum calcium concentration and $1,25(OH)_2D_3$ level were significantly higher in the sham and treatment groups compared with the GIOP group (both $P<0.05$; Table II). The serum alkaline phosphatase level was significantly lower in the sham and treatment groups than that in the GIOP group (both $P<0.05$; Table II). No significant difference was observed in the serum phosphorous levels among the three groups (Table II).

Comparison of 3D micro-CT imaging parameters. 3D reconstruction of the third lumbar vertebra samples indicated markedly attenuated bone density, severely impaired bone micro-architecture, thinner and reduced-density trabeculae and reduced connectivity in the GIOP group compared with those in the sham group (Fig. 1). Rod-like trabeculae outnumbered plate-like structures and larger inter-trabecular spaces were observed in the GIOP group compared with the sham group (Fig. 1). Additionally, bone volume/total tissue volume, trabecular number and trabecular thickness decreased significantly and structure model index, trabecular spacing and bone surface to bone volume ratio increased significantly in the GIOP group compared with sham group (all $P<0.05$; Fig. 1). These results indicate that the experimental model was effective.

The third lumbar vertebra and femur bone structure was markedly improved in both the treatment and sham groups compared with the GIOP group. This superiority was demonstrated by a large number of parallel trabeculae arranged in the same direction, lower porosity and a significantly increased bone volume/total tissue volume, trabecular number and trabecular thickness compared with those in the GIOP group (all $P<0.05$; Figs. 1 and 2). However, the structure model index, trabecular spacing and bone surface to bone volume ratio were

Table II. Effects of $1,25(OH)_2D_3$ supplementation on body weight, Ca, Pi, ALP and $1,25(OH)_2D_3$ levels in mice.

Group	Body weight	Ca (mg/dl)	Pi (mg/dl)	ALP (IU/l)	$1,25(OH)_2D_3$ (pmol/l)
Sham	30.91±2.01[a]	7.38±0.87[a]	6.55±0.32	69.65±5.16[a]	172.62±15.16[a]
Treatment	32.38±2.44[a]	7.63±0.92[a]	6.85±0.57	73.33±11.35[a]	189.33±17.36[a,b]
GIOP	38.52±2.93	4.96±0.53	6.76±0.26	130.43±13.32	145.18±12.83

All data were evaluated by Tukey's multiple comparison test and are presented as the mean ± standard deviation (n=12 in both sham and treatment groups; n=11 in GIOP group). [a]P<0.05 vs. the GIOP group; [b]P<0.05 vs. the sham group. $1,25(OH)_2D_3$, 1,25-dihydroxyvitamin D_3; GIOP, glucocorticoid-induced osteoporosis; Ca, serum calcium; Pi, inorganic-phosphorous; ALP, alkaline phosphatase.

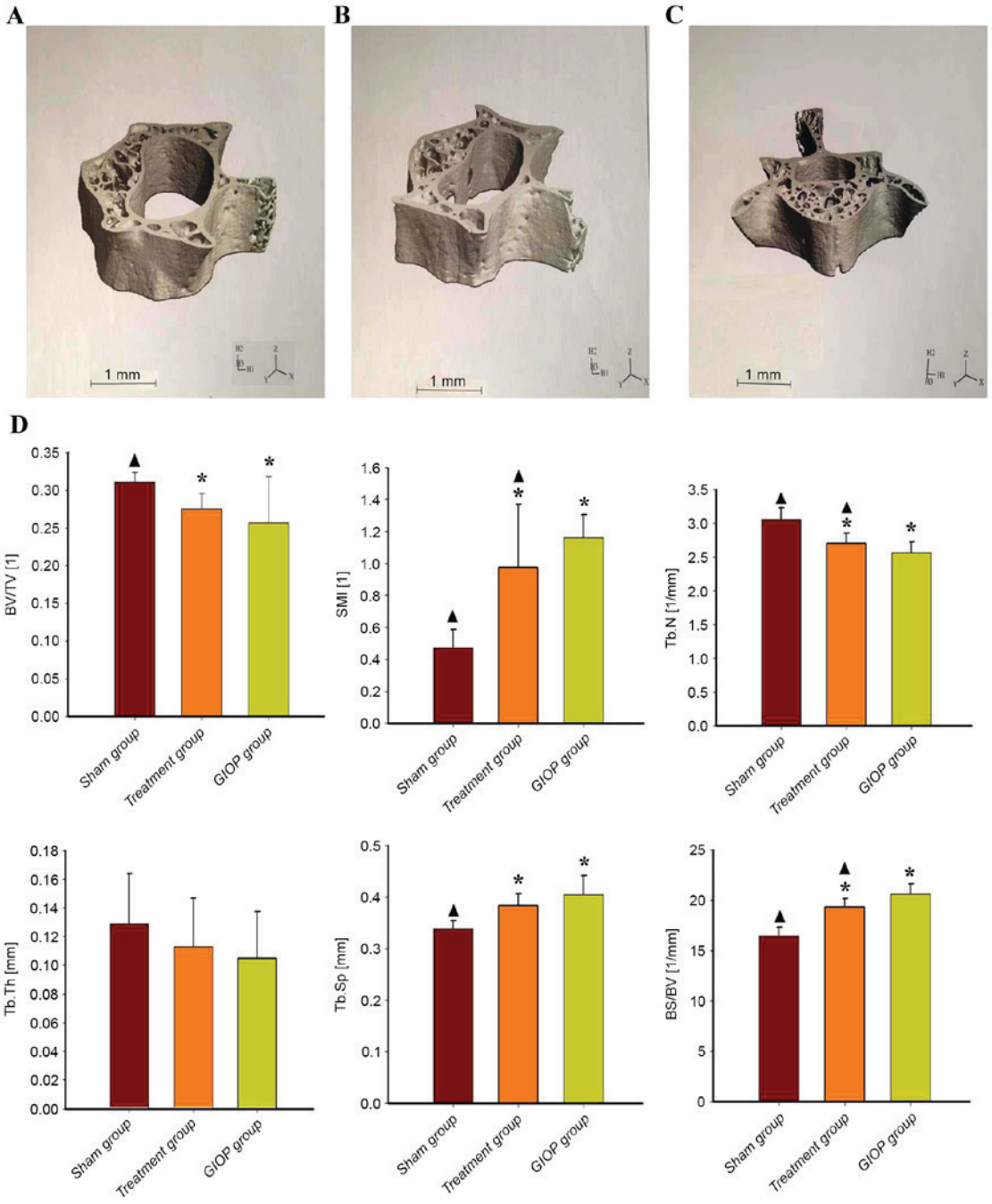

Figure 1. Micro-CT and bone morphometric parameters for the third lumbar vertebra for the three groups. Micro-CT images of the third lumbar vertebra from the (A) sham, (B) $1,25(OH)_2D_3$ treatment and (C) GIOP groups. (D) Bone morphometric parameters of the third lumbar vertebra from the three groups. Data are presented as the mean ± standard deviation. *P<0.05 vs. the sham group; ▲P<0.05 vs. the GIOP group. CT, computed tomography; GIOP, glucocorticoid-induced osteoporosis; BV, bone volume; TV, total tissue volume; Tb.N, trabecular number; Tb.Th, trabecular thickness; Tb.Sp, trabecular spacing; SMI, structure model index; BV/TV, bone volume to total tissue volume ratio (bone volume fraction); BS/BV, bone surface to bone volume ratio.

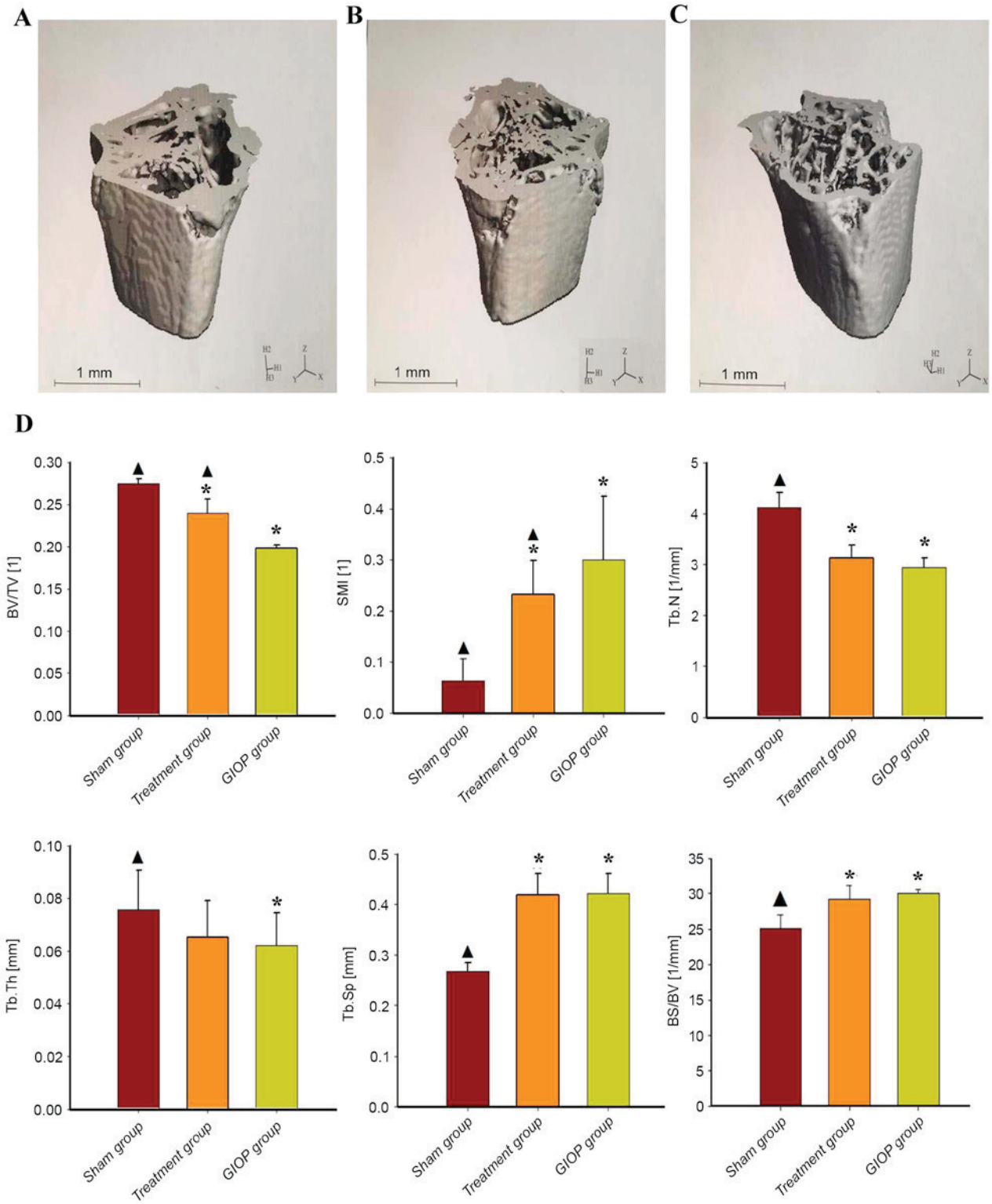

Figure 2. Micro-CT and bone morphometric parameters of the femur for the three groups. Micro-CT images of the femur from the (A) sham, (B) $1,25(OH)_2D_3$ treatment and (C) GIOP groups. (D) Bone morphometric parameters of the femur from the three groups. Data are presented as the mean ± standard deviation. *P<0.05 vs. the sham group; ▲P<0.05 vs. the GIOP group. CT, computed tomography; GIOP, glucocorticoid-induced osteoporosis; BV, bone volume; TV, total tissue volume; Tb.N, trabecular number; Tb.Th, trabecular thickness; Tb.Sp, trabecular spacing; SMI, structure model index; BV/TV, bone volume to total tissue volume ratio (bone volume fraction); BS/BV, bone surface to bone volume ratio.

significantly lower in the control group than in the GIOP group (all P<0.05; Figs. 1 and 2).

Expression of bone turnover markers, major RAS components, OPG and RANKL in the circulating and local mRNA and/or protein. Expression levels of bone turnover markers, β-CTX and T-PINP, in the treatment and sham groups were significantly lower than those in the GIOP group (P<0.05; Fig. 3). No significant differences were detected between the treatment and sham groups (Fig. 3). Additionally, there were

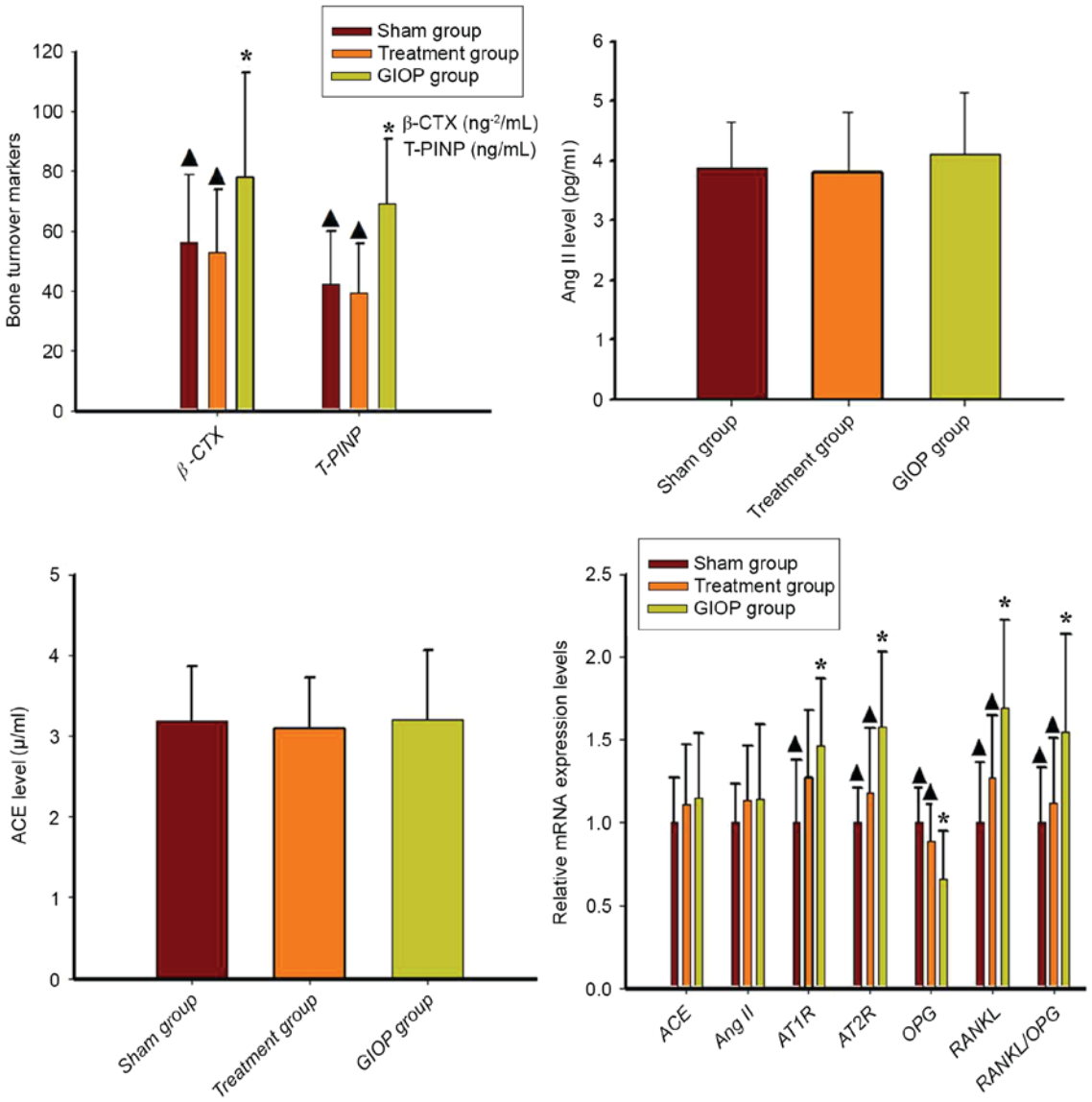

Figure 3. Circulating levels and local bone mRNA expression levels of the renin-angiotensin system and bone turnover markers in the three groups. Data are presented as the mean ± standard deviation. *P<0.05 vs. the sham group; ▲P<0.05 vs. the GIOP group. AT1R, angiotensin type 1 receptor; AT2R, angiotensin type 2 receptor; ACE, angiotensin-converting enzyme; Ang II, angiotensin II; GIOP, glucocorticoid-induced osteoporosis; β-CTX, β-Crosslaps; OPG, osteoprotegerin; RANKL, receptor activator of nuclear factor-kB ligand; T-PINP, total N-terminal propeptide of type I procollagen.

no significant differences in circulating levels of ACE and Ang II among the three groups (P>0.05; Fig. 3).

In the lumbar vertebrae, mRNA expression levels of *AT1R*, *AT2R* and *RANKL* and the *RANKL*/*OPG* ratio were significantly higher in the GIOP group than in the sham group (P<0.05; Fig. 3). However, compared with the GIOP group, the mRNA expression levels of *AT2R* and *RANKL* and the *RANKL*/*OPG* ratio in lumbar vertebrae were significantly lower in the treatment group (P<0.05; Fig. 3). Furthermore, immunohistochemical staining revealed that AT1R and ACE were expressed in osteoblasts, osteoclasts and bone marrow cells; however, they were not expressed in osteocytes (Fig. 4).

Discussion

The present study demonstrated that the bone conversion index, represented by β-CTX and T-PINP levels, in GIOP mice was significantly higher than in the sham group, indicating that the GIOP mice were exhibiting high bone turnover, which leads to bone loss. The results of micro-CT imaging and immunohistochemical staining demonstrated the therapeutic effect of $1,25(OH)_2D_3$ in a murine model of GIOP (26).

It has previously been reported that an absence of vitamin D signaling in mice lacking the VDR gene resulted in an increase in renin gene expression and circulating Ang II levels (27). However, in the present study, the lack of an increase in Ang II concentration and ACE activity in the circulatory system with $1,25(OH)_2D_3$ treatment suggests that the dose of $1,25(OH)_2D_3$ used did not influence the circulatory systemic RAS. This may be due to the homeostatic regulation of $1,25(OH)_2D_3$ levels, which caused individuals to exhibit the same normal range of $1,25(OH)_2D_3$ in the treatment group and GIOP group. Notably, in the present study, the Ang II concentration and ACE activity in the circulatory system were not significantly different

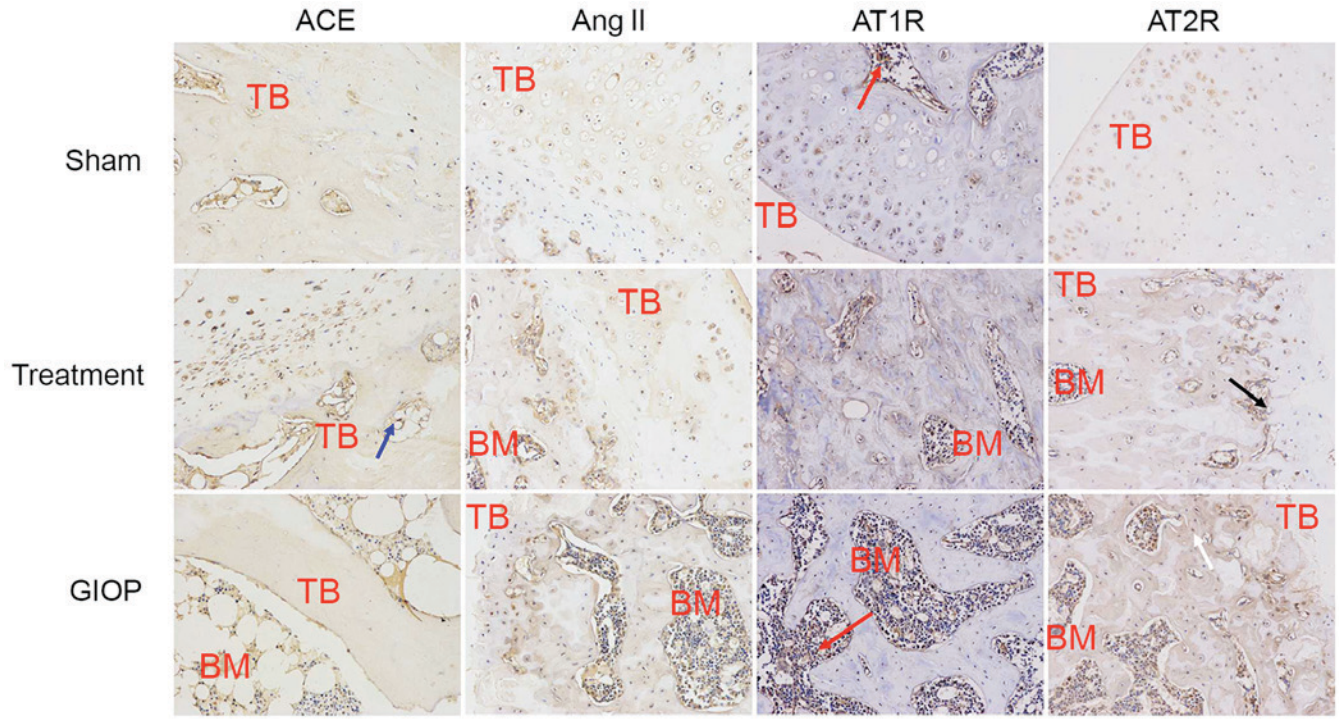

Figure 4. Immunohistochemical staining of ACE, Ang II, AT1R and AT2R in the three groups (magnification, x200). ACE, Ang II, AT1R and AT2R were expressed in osteoclasts (white arrows), osteoblasts (red arrows) and bone marrow cells (black arrows); however, they were not expressed in osteocytes (blue arrows) in lumbar vertebrae. ACE, angiotensin-converting enzyme; Ang II, angiotensin II; AT1R, angiotensin type 1 receptor; AT2R, angiotensin type 2 receptor; GIOP, glucocorticoid-induced osteoporosis; BM, bone marrow; TB, trabecular bone.

between the GIOP and sham groups. Previous research has reported that feeding cholesterol to rabbits increased local tissue, while not serum, ACE activity (27). This difference between the local tissue and the systemic RAS may be a consequence of a greater stability of systemic RAS following exogenous stimulation.

Analysis of bone immunohistochemistry and biochemical markers suggested that GIOP predominantly inhibited bone formation and enhanced bone resorption in the present study. This finding is supported by previous studies (28,29). The present study demonstrated that high bone turnover increased the RANKL/OPG ratio, followed by activation of the local bone RAS, which is supported by previous research (22). Additionally, the present study indicated that GIOP increased osteoclast number and activity. Many studies have indicated that Ang II is a potent stimulator of osteoclastic bone resorption (30-34). Ang II also promotes osteoclast differentiation and activation indirectly by binding to different osteoblast receptors whilst upregulating RANKL expression (22). A study by Shimizu *et al* (10) demonstrated that Ang II induced RANKL expression directly in osteoblasts by activating AT1R, which may explain why AT1R inhibitors reduce fracture risk in older adults (35-38). Nevertheless, previous research has revealed that Ang II induces RANKL expression via AT2R (11). Overall, these results are consistent with the finding that the bone conversion index in GIOP mice was higher than that in control mice in the present study.

A study by Zhang *et al* (39) reported that vitamin D was able to inhibit RAS activity in the kidney, improve renal function and prevent the occurrence of nephritis and fibrosis in mice caused by long-term hyperglycemia or unilateral ureteral obstruction. In the present study, $1,25(OH)_2D_3$ treatment improved the quality of cancellous bone in GIOP mice by inhibiting local RAS activity in bone tissue through a reduction in the generation of Ang II, thus downregulating the expression of osteoclast factors that may reduce bone resorption activity. A previous study provided evidence that local RAS is related to bone mineral density in GIOP patients (22).

One strength of the present study was that it utilized murine bone tissue and micro-CT to detect changes. However, a limitation was that the measurement of aldosterone was not performed, which is associated with the renin-angiotensin-aldosterone system. Nevertheless, the present study raises some important questions, such as whether $1,25(OH)_2D_3$ increased bone mineral density by inhibiting the local RAS and modulating the RANKL/OPG ratio in bone. Results of the present study should therefore trigger future clinical research to investigate these relationships further.

In conclusion, $1,25(OH)_2D_3$ treatment may improve skeletal complications resulting from GC therapy. To the best of our knowledge, this is the first study on the efficacy of $1,25(OH)_2D_3$ for maintaining healthy bones by influencing the RAS in local bone tissue, suggesting a novel angle for the understanding of the mechanisms involved in the protection of bone by $1,25(OH)_2D_3$.

Acknowledgements

The present study was partially funded by the National Natural Science Foundation of China (grant nos. 81403257 and 81473492).

References

1. van Staa TP, Geusens P, Pols HA, de Laet C, Leufkens HG and Cooper C: A simple score for estimating the long-term risk of fracture in patients using oral glucocorticoids. QJM 98: 191-198, 2005.
2. van Staa TP: The pathogenesis, epidemiology and management of glucocorticoid-induced osteoporosis. Calcif Tissue Int 79: 129-137, 2006.
3. Rizzoli R, Adachi JD, Cooper C, Dere W, Devogelaer JP, Diez-Perez A, Kanis JA, Laslop A, Mitlak B, Papapoulos S, *et al*: Management of glucocorticoid-induced osteoporosis. Calcif Tissue Int 91: 225-243, 2012.
4. Lekamwasam S, Adachi JD, Agnusdei D, Bilezikian J, Boonen S, Borgström F, Cooper C, Diez Perez A, Eastell R, Hofbauer LC, *et al*: A framework for the development of guidelines for the management of glucocorticoid-induced osteoporosis. Osteoporos Int 23: 2257-2276, 2012.
5. Llorens-Cortes C and Kordon C: Jacques benoit lecture: The neuroendocrine view of the angiotensin and apelin systems. J Neuroendocrinol 20: 279-289, 2008.
6. Kalupahana NS and Moustaid-Moussa N: The renin-angiotensin system: A link between obesity, inflammation and insulin resistance. Obes Rev 13: 136-149, 2012.
7. Hagiwara H, Hiruma Y, Inoue A, Yamaguchi A and Hirose S: Deceleration by angiotensin II of the differentiation and bone formation of rat calvarial osteoblastic cells. J Endocrinol 156: 543-550, 2008.
8. Hatton R, Stimpel M and Chambers TJ: Angiotensin II is generated from angiotensin I by bone cells and stimulates osteoclastic bone resorption in vitro. J Endocrinol 152: 5-10, 1997.
9. Liu YY, Yao WM, Wu T, Xu BL, Chen F and Cui L: Captopril improves osteopenia in ovariectomized rats and promotes bone formation in osteoblasts. J Bone Miner Metab 29: 149-158, 2011.
10. Shimizu H, Nakagami H, Osako MK, Hanayama R, Kunugiza Y, Kizawa T, Tomita T, Yoshikawa H, Ogihara T and Morishita R: Angiotensin II accelerates osteoporosis by activating osteoclasts. FASEB J 22: 2465-2475, 2008.
11. Asaba Y, Ito M, Fumoto T, Watanabe K, Fukuhara R, Takeshita S, Nimura Y, Ishida J, Fukamizu A and Ikeda K: Activation of renin-angiotensin system induces osteoporosis independently of hypertension. J Bone Miner Res 24: 241-250, 2009.
12. Xiang W, Kong J, Chen S, Cao LP, Qiao G, Zheng W, Liu W, Li X, Gardner DG and Li YC: Cardiac hypertrophy in vitamin D receptor knockout mice: Role of the systemic and cardiac renin-angiotensin systems. Am J Physiol Endocrinol Metab 288: E125-E132, 2005.
13. Zhou C, Lu F, Cao K, Xu D, Goltzman D and Miao D: Calcium-independent and 1,25(OH)2D3-dependent regulation of the renin-angiotensin system in 1alpha-hydroxylase knockout mice. Kidney Int 74: 170-179, 2008.
14. Tomaschitz A, Pilz S, Ritz E, Grammer T, Drechsler C, Boehm BO and März W: Independent association between 1,25-dihydroxyvitamin D, 25-hydroxyvitamin D and the renin-angiotensin system: The Ludwigshafen Risk and Cardiovascular Health (LURIC) study. Clin Chim Acta 411: 1354-1360, 2010.
15. Yuan W, Pan W, Kong J, Zheng W, Szeto FL, Wong KE, Cohen R, Klopot A, Zhang Z and Li YC: 1,25-dihydroxyvitamin D3 suppresses renin genetranscription by blocking the activity of the cyclic AMP response element in the renin gene promoter. J Biol Chem 282: 29821-29830, 2007.
16. Li YC, Kong J, Wei M, Chen ZF, Liu SQ and Cao LP: 1,25-Dihydroxyvitamin D(3) is a negative endocrine regulator of the renin-angiotensin system. J Clin Invest 110: 229-238, 2002.
17. Yuan W, Pan W, Kong J, Zheng W, Szeto FL, Wong KE, Cohen R, Klopot A, Zhang Z and Li YC: 1,25-dihydroxyvitamin D3 suppresses renin genetranscription by blocking the activity of the cyclic AMP response element in the renin gene promoter. J Biol Chem 282: 29821-29830, 2007.
18. Contrera JF, Matthews EJ, Kruhlak NL and Benz RD: Estimating the safe starting dose in phase I clinical trials and no observed effect level based on QSAR modeling of the human maximum recommended daily dose. Regul Toxicol Pharmacol 40: 185-206, 2004.
19. Ruegsegger P, Koller B and Müller R: A microtomographic system for the nondestructive evaluation of bone architecture. Calcif Tissue Int 58: 24-29, 1996.
20. Shuai B, Shen L, Yang Y, Ma C, Zhu R and Xu X: Assessment of the impact of zoledronic acid on ovariectomized osteoporosis model using Micro-CT scanning. PLoS One 10: e0132104, 2015.
21. Ito M, Nakamura T, Matsumoto T, Tsurusaki K and Hayashi K: Analysis of trabecular microarchitecture of human iliac bone using microcomputed tomography in patients with hip arthrosis with or without vertebral fracture. Bone 23: 163-169, 1998.
22. Shuai B, Yang YP, Shen L, Zhu R, Xu XJ, Ma C, Lv L, Zhao J and Rong JH: Local renin-angiotensin system is associated with bone mineral density of glucocorticoid-induced osteoporosis patients. Osteoporos Int 26: 1063-1071, 2015.
23. Livak KJ and Schmittgen TD: Analysis of relative gene expression data using real-time quantitative PCR and the 2-(Delta Delta C(T)) method. Methods 25: 402-408, 2001.
24. Yang YP, Shuai B, Shen L, Xu XJ, Ma C and Lv L: Effect of Qing'e formula on circulating sclerostin levels in patients with postmenopausal osteoporosis. J Huazhong Univ Sci Technol Med Sci 35: 645-648, 2015.
25. Shuai B, Shen L, Zhu R and Zhou PQ: Effect of Qing'e formula on the in vitro differentiation of bone marrow-derived mesenchymal stem cells from proximal femurs of postmenopausal osteoporotic mice. BMC Complement Altern Med 15: 250, 2015.
26. Kinney JH, Haupt DL, Balooch M, Ladd AJ, Ryaby JT and Lane NE: Three-dimensional morphometry of the L6 vertebra in the ovariectomized rat model of osteoporosis: Biomechanical implications. J Bone Miner Res 15: 1981-1991, 2000.
27. Donmez BO, Ozdemir S, Sarikanat M, Yaras N, Koc P, Demir N, Karayalcin B and Oguz N: Effect of angiotensin II type 1 receptor blocker on osteoporotic rat femurs. Pharmacol Rep 64: 878-888, 2012.
28. Pérez-Castrillón JL, Justo I, Silva J, Sanz A, Martín-Escudero JC, Igea R, Escudero P, Pueyo C, Diaz C, Hernández G and Dueñas A: Relationship between bone mineral density and angiotensin converting enzyme polymorphism in hypertensive postmenopausal women. Am J Hypertens 16: 233-235, 2003.
29. Woods D, Onambele G, Woledge R, Skelton D, Bruce S, Humphries SE and Montgomery H: Angiotensin-I converting enzyme genotype-dependent benefit from hormone replacement therapy in isometric muscle strength and bone mineral density. J Clin Endocrinol Metab 86: 2200-2204, 2001.
30. Lynn H, Kwok T, Wong SY, Woo J and Leung PC: Angiotensin converting enzyme inhibitor use is associated with higher bone mineral density in elderly Chinese. Bone 38: 584-388, 2006.
31. Rejnmark L, Vestergaard P and Mosekilde L: Treatment with beta-blockers, ACE inhibitors, and calcium-channel blockers is associated with a reduced fracture risk: A nationwide case-control study. J Hypertens 24: 581-589, 2006.
32. Garcia P, Schwenzer S, Slotta JE, Scheuer C, Tami AE, Holstein JH, Histing T, Burkhardt M, Pohlemann T and Menger MD: Inhibition of angiotensin-converting enzyme stimulates fracture healing and periosteal callus formation-role of a local renin-angiotensin system. Br J Pharmacol 159: 1672-1680, 2010.
33. Izu Y, Mizoguchi F, Kawamata A, Hayata T, Nakamoto T, Nakashima K, Inagami T, Ezura Y and Noda M: Angiotensin II type 2 receptor blockade increases bone mass. J Biol Chem 284: 4857-4864, 2009.
34. Haznedaroglu IC and Oztürk MA: Towards the understanding of the local hematopoietic bone marrow renin-angiotensin system. Int J Biochem Cell Biol 35: 867-880, 2003.
35. Bergula AP, Huang W and Frangos JA: Femoral vein ligation increases bone mass in the hindlimb suspended rat. Bone 24: 171-177, 1999.
36. McCarthy ID: Fluid shifts due to microgravity and their effects on bone: A review of current knowledge. Ann Biomed Eng 33: 95-103, 2005.
37. Solomon DH, Mogun H, Garneau K and Fischer MA: Risk of fractures in older adults using antihypertensive medications. J Bone Miner Res 26: 1561-1567, 2011.
38. Yonqtao Z, Kunzheng W, Jingjing Z, Hu S, Jianqiang K, Ruiyu L and Chunsheng W: Glucocorticoids activate the local renin-angiotensin system in bone: Possible mechanism for glucocorticoid-induced osteoporosis. Endocrine 47: 598-608, 2014.
39. Zhang FY, Yang FJ, Yang JL, Wang L and Zhang Y: Renin inhibition improves ovariectomy-induced steoporosis of lumbar vertebra in mice. Biol Pharm Bull 37: 1994-1997, 2014.